

Contribution from the Laboratorium für Anorganische Chemie, ETH-Zentrum, CH-8092 Zürich, Switzerland, Institut für Kristallographie und Petrographie, ETH-Zentrum, CH-8092 Zürich, Switzerland, and Anorganisch-Chemisches Institut der Universität Zürich, Winterthurerstrasse 190, CH-8057 Zürich, Switzerland

Preparation of Complexes Containing the $[\text{Mo}_3\text{S}(\text{S}_2)_3]^{4+}$ Core and Structure of Tris(diethyldithiocarbamato)tris(μ -disulfido)(μ_3 -thio)-triangulo-trimolybdenum(IV) Iodide

Heinrich Zimmermann,^{1a} Kaspar Hegetschweiler,^{*,1a} Thomas Keller,^{1a} Volker Gramlich,^{1b} Helmut W. Schmalle,^{1c} Walter Petter,^{1b} and Walter Schneider^{1a}

Received April 23, 1991

A variety of complexes containing the core $\text{Mo}_3\text{S}(\text{S}_2)_3$ have been prepared by using two different synthetic pathways. The ligands diethyldithiocarbamate (dte^-), 8-hydroxyquinoline (Hoxq), 2-thiopyridine (Htpy), and catechol (H_2cat) were used. $[\text{Mo}_3\text{S}(\text{S}_2)_3(\text{dte})_3]\text{I}$, $[\text{Mo}_3\text{S}(\text{S}_2)_3(\text{tpy})_3]\text{I}$, and $[\text{Mo}_3\text{S}(\text{S}_2)_3(\text{tpy})_2(\text{dte})]\text{I}$ were prepared by the oxidation of the terminal disulfido groups of $[\text{Mo}_3\text{S}(\text{S}_2)_6]^{2-}$ with the disulfides dte_2 and tpy_2 . Both, the absence of a reaction with cystine and the decrease of the reaction rate according to $\text{dte}_2 > \text{tpy}_2 \gg \text{cystine}$ are discussed in terms of the influence of the redox potential on the reaction rate. $[\text{Mo}_3\text{S}(\text{S}_2)_3(\text{oxq})_3]\text{Br}$, $(\text{PPh}_4)_2[\text{Mo}_3\text{S}(\text{S}_2)_3(\text{cat})_3]$, and $[\text{Mo}_3\text{S}(\text{S}_2)_3(\text{dte})_3]\text{X}$ ($\text{X} = \text{I}, \text{Br}$) were obtained by the substitution of Br^- in $[\text{Mo}_3\text{S}(\text{S}_2)_3\text{Br}_6]^{2-}$. Two types of crystals of the polymorphous $[\text{Mo}_3\text{S}(\text{S}_2)_3(\text{dte})_3]\text{I}$ have been analyzed by X-ray diffraction, modification 1 with space group Aba2 , $Z = 8$, $a = 24.92$ (2) Å, $b = 17.93$ (1) Å, and $c = 16.56$ (1) Å and modification 2 with space group Iba2 , $Z = 8$, $a = 17.761$ (3) Å, $b = 24.281$ (4) Å, and $c = 16.74$ (1) Å. In both crystals, a weak binding of I^- to the three axial sulfur atoms of the complex was found, with average distance $\text{I}-\text{S}$ of 3.30 Å (modification 1) and 3.25 Å (modification 2). According to similar structures described in literature, a general anionic binding site of $[\text{Mo}_3\text{S}(\text{S}_2)_3]^{4+}$ is postulated. In the FAB mass spectrum of $[\text{Mo}_3\text{S}(\text{S}_2)_3(\text{tpy})_2(\text{dte})]$ a redistribution of ligands was indicated by the signals of $[\text{Mo}_3\text{S}(\text{S}_2)_3(\text{tpy})_x(\text{dte})_y]$ ($3 \geq x \geq 1$, $2 \geq y \geq 0$). On the other hand, no dissociation of dte has been detected in solutions of $[\text{Mo}_3\text{S}_7(\text{dte})_3]\text{I}$ at room temperature by NMR spectroscopy. However, the signals of the free Hoxq and H_2cat , as observed in the ^1H NMR spectrum of $[\text{Mo}_3\text{S}_7(\text{oxq})_3]^+$ and $[\text{Mo}_3\text{S}_7(\text{cat})_3]^{2-}$, indicated more labile $\text{Mo}-\text{N}$ and $\text{Mo}-\text{O}$ bonds compared to the $\text{Mo}-\text{S}$ bond in the dte complex.

Introduction

Although the first compound containing the cluster core $[\text{Mo}_3\text{S}(\text{S}_2)_3]^{4+}$ was already discovered in 1974,² only a limited number of complexes with this core have been prepared subsequently.³⁻⁷ It has been demonstrated that this core is surprisingly inert against attack by strong acid and oxidizing agents^{8,9} whereas in the presence of nucleophilic agents the degradation to $[\text{Mo}_3\text{S}(\text{S})_3]^{4+}$ is observed.^{6,10} The influence of peripheral ligands on the reactivity of $[\text{Mo}_3\text{S}(\text{S}_2)_3]^{4+}$ complexes has not been investigated so far. To elucidate the different properties of such complexes as a function of their periphery, a representative series is required and efficient synthetic pathways are needed. In the present work, we present the preparation and characterization of a variety of complexes of $[\text{Mo}_3\text{S}(\text{S}_2)_3]^{4+}$ with the bidentate ligands catechol (H_2cat), 8-hydroxyquinoline (Hoxq), 2-thiopyridine (Htpy), and diethyldithiocarbamate (dte) providing O, N, and S atoms as binding sites for Mo. For the preparation of the complexes, the easily obtainable $(\text{NH}_4)_2[\text{Mo}_3\text{S}(\text{S}_2)_6]$ and $(\text{NEt}_4)_2[\text{Mo}_3\text{S}(\text{S}_2)_3\text{Br}_6]$ were used as starting materials.

$[\text{Mo}_3\text{S}(\text{S}_2)_6]^{2-}$ is a remarkable species with bridging and terminal disulfido groups in the same molecule.³ It has been reported recently that the terminal disulfido groups are selectively oxidized by halogens X_2 to $[\text{Mo}_3\text{S}(\text{S}_2)_5\text{X}_2]^{2-}$ ($\text{X} = \text{Cl}, \text{Br}$).⁸ In this investigation, the analogous oxidation of $[\text{Mo}_3\text{S}(\text{S}_2)_6]^{2-}$ by the organic disulfides tetraethylthiuram disulfide (dte_2) and 2,2'-di-thiodipyrindine (tpy_2) is described, resulting in novel complexes of the $[\text{Mo}_3\text{S}(\text{S}_2)_3]^{4+}$ core.

The reactivity of $[\text{Mo}_3\text{S}(\text{S}_2)_3\text{Br}_6]^{2-}$ with nucleophilic agents has been studied by Fedin et al. and in our laboratory.^{8,9} Two different reaction types were discovered: Monodentate and bidentate phosphines attack the bridging disulfido groups in the same way as observed for $[\text{Mo}_3\text{S}(\text{S}_2)_6]^{2-}$, leading to derivatives of $[\text{Mo}_3\text{S}_4]^{4+}$ where some of the Br atoms are still bound to Mo.⁸ However, in the presence of 2-mercaptosuccinic acid and 2-mercaptobenzoic acid, substitution of the six Br^- ions took place under complete preservation of the $[\text{Mo}_3\text{S}(\text{S}_2)_3]^{4+}$ core.⁹ We used additional bidentate N,O,S ligands as nucleophilic agents for $[\text{Mo}_3\text{S}(\text{S}_2)_3\text{Br}_6]^{2-}$ to establish this substitution reaction as a general synthetic pathway.

The mass spectra of some of the new $[\text{Mo}_3\text{S}(\text{S}_2)_3]^{4+}$ complexes presented here have been discussed previously.¹¹ This contribution is a comprehensive report on the preparation and structural characterization of the new compounds.

Experimental Section

Instrumentation and Physical Measurements. The UV-vis spectra were recorded on an Uvikon 820 spectrophotometer, IR spectra were measured on a Beckman IR-4250 spectrometer (CsI wafer), and the ^1H and ^{13}C NMR spectra were obtained by using Bruker AC-200 and Bruker WM-250 spectrometers, with a δ (ppm) scale and TMS ($=0$ ppm) as an internal standard. The FAB-MS spectra were run on a VG ZAB-VSEQ instrument, and the magnetic susceptibility was measured on a magnetic susceptibility balance (Johnson Matthey) at room temperature.

Materials and Methods. $(\text{NH}_4)_2[\text{Mo}_3\text{S}(\text{S}_2)_6]$ was obtained by the method given by Müller,¹² $(\text{NEt}_4)_2[\text{Mo}_3\text{S}_7\text{Br}_6]$ was prepared as described earlier.⁹ $(\text{PPh}_4)_2[\text{Mo}_3\text{S}_7\text{Br}_6]$ was synthesized by the same procedure, using PPh_4Br instead of NEt_4Br for precipitation. All other reagents

- (1) (a) Laboratorium für Anorganische Chemie, ETH Zürich. (b) Institut für Kristallographie und Petrographie, ETH Zürich. (c) Anorganisch-Chemisches Institut der Universität Zürich.
- (2) Marcoll, J.; Rabenau, A.; Mootz, D.; Wunderlich, H. *Rev. Chim. Miner.* **1974**, *11*, 607.
- (3) Müller, A.; Pohl, S.; Dartmann, M.; Cohen, J. P.; Benett, J. M.; Kirchner, R. M. *Z. Naturforsch.* **1979**, *34B*, 434.
- (4) Meyer, B.; Wunderlich, H. *Z. Naturforsch.* **1982**, *37B*, 1437.
- (5) Maoyu, B. S.; Jinling, H.; Jiaxi, L. *Acta Crystallogr.* **1984**, *C40*, 759.
- (6) Halbert, T. R.; McGauley, K.; Pan, W.-H.; Scernuszewicz, R. S.; Stiefel, E. I. *J. Am. Chem. Soc.* **1984**, *106*, 1849.
- (7) Klingelhöfer, P.; Müller, U.; Friebe, C.; Pebler, J. *Z. Anorg. Allg. Chem.* **1986**, *543*, 22.
- (8) Fedin, V. P.; Sokolov, M. N.; Mironov, Y. V.; Kolesov, B. A.; Tkachev, S. V.; Fedorov, V. Y. *Inorg. Chim. Acta* **1990**, *167*, 39.
- (9) Hegetschweiler, K.; Keller, T.; Zimmermann, H.; Schneider, W.; Schmalle, H.; Dubler, E. *Inorg. Chim. Acta* **1990**, *169*, 235.
- (10) (a) Müller, A.; Reinsch, U. *Angew. Chem.* **1980**, *92*, 69. (b) Keck, H.; Kuchen, W.; Mathow, J.; Wunderlich, H. *Angew. Chem.* **1982**, *94*, 927. (c) Cotton, F. A.; Llugar, R.; Marler, D. O.; Schwotzer, W. *Inorg. Chim. Acta* **1985**, *102*, L25.
- (11) Hegetschweiler, K.; Keller, T.; Amrein, W.; Schneider, W. *Inorg. Chem.* **1991**, *30*, 873.
- (12) Müller, A.; Bhattacharyya, R. G.; Pfefferkorn, B. *Chem. Ber.* **1979**, *112*, 778.

* To whom correspondence should be addressed.

were commercially available products of reagent grade quality.

Analyses. Mo was determined photometrically as bis(tironato)-molybdenum(VI) (390 nm) after digestion of the sample by aqua regia. C, H, and N analyses were performed by D. Manser, Laboratorium für Organische Chemie, ETH, Zürich, Switzerland.

Preparation of $[\text{Mo}_3\text{S}_7(\text{dtc})_3]\text{I}$ (Modification 1). $(\text{NH}_4)_2[\text{Mo}_3\text{S}(\text{S}_2)_6]$ (0.30 g in 30 mL of DMF) and dtc_2 (0.40 g in 10 mL of DMF) were mixed and allowed to stay for 30 min at room temperature. The solution was then heated to 50 °C, and NaI (2 g in 50 mL of EtOH) was added. After the solution was cooled to room temperature, an orange solid precipitated, which was recrystallized from $\text{CH}_2\text{Cl}_2/\text{EtOH}$ and dried in vacuo. Yield: 0.38 g (85%). UV/vis: No maximum above 260 nm. Anal. Calc for $\text{C}_{15}\text{H}_{30}\text{N}_3\text{S}_{13}\text{Mo}_3\text{I}$: C, 16.61; H, 2.79; N, 3.88; Mo, 26.55; I, 11.71. Found: C, 16.44; H, 2.83; N, 3.93; Mo, 26.56; I, 11.52. A solution in CH_2Cl_2 was filtered and layered with hexane. In this way, yellow crystals of a characteristic triangular shape, suitable for X-ray analysis, were obtained.

Preparation of $[\text{Mo}_3\text{S}_7(\text{dtc})_3]\text{I}$ (Modification 2). $(\text{NEt}_4)_2[\text{Mo}_3\text{S}_7\text{Br}_6]$ (0.5 g) was dissolved in DMF (40 mL, 70 °C), and solid Na(dtc) (0.35 g) was added. The solution was kept at 70 °C until the color changed to deep brown. The addition of NaI (2.05 g in EtOH) and 100 mL of ether resulted in the precipitation of a white solid. The solid was filtered off, and the clear brown solution was allowed to stay at 4 °C for several days. Large brown crystals were obtained, which could be used for X-ray diffraction without further purification. Anal. Calc for $\text{C}_{15}\text{H}_{30}\text{N}_3\text{S}_{13}\text{Mo}_3\text{I}$: C, 16.61; H, 2.79; N, 3.88. Found: C, 16.80; H, 2.83; N, 3.98.

Preparation of $[\text{Mo}_3\text{S}_7(\text{dtc})_3]\text{Br}$. $(\text{NEt}_4)_2[\text{Mo}_3\text{S}_7\text{Br}_6]$ (1.3 g) was dissolved in CH_3CN (150 mL, 70 °C), and Na(dtc) (0.93 g, dissolved in 30 mL of CH_3CN) was then added in several portions. After the addition, which caused the precipitation of a solid, the suspension was stirred for 20 min at 70 °C. After the solution was cooled to 50 °C, the orange solid was filtered out and recrystallized from hexane/ CH_2Cl_2 . Yield: 0.6 g (56%). Anal. Calc for $\text{C}_{15}\text{H}_{30}\text{N}_3\text{S}_{13}\text{Mo}_3\text{Br}$: C, 17.37; H, 2.92; N, 4.05; Mo, 27.76. Found: C, 17.0; H, 2.71; N, 3.90; Mo, 27.67.

Preparation of $[\text{Mo}_3\text{S}_7(\text{tpy})_3]\text{I} \cdot \text{CH}_2\text{Cl}_2$ and $[\text{Mo}_3\text{S}_7(\text{tpy})_2(\text{dtc})]\text{I}$. $(\text{NH}_4)_2[\text{Mo}_3\text{S}(\text{S}_2)_6]$ (0.80 g) and tpy_2 (1.19 g) were dissolved in 30 mL of DMF, and the solution was stirred for 20 h at 110 °C. The solution was then cooled to room temperature and filtered. A clear orange solution (1) and a black solid (2) were obtained.

The orange solution (1) was heated to 50 °C, and NaI (3 g, dissolved in 20 mL of EtOH, 50 °C) was added. An orange solid precipitated, which was filtered out and dried in vacuo. Yield: 0.12 g (11%) of $[\text{Mo}_3\text{S}_7(\text{tpy})_3]\text{I} \cdot \text{CH}_2\text{Cl}_2$. UV/vis: No maximum above 260 nm. Anal. Calc for $\text{C}_{16}\text{H}_{14}\text{N}_3\text{S}_{10}\text{Cl}_2\text{Mo}_3\text{I}$: C, 18.22; H, 1.34; N, 3.98; Mo, 27.29; I, 12.03. Found: C, 18.27; H, 1.27; N, 3.96; Mo, 27.57; I, 12.06.

A 0.3-g amount of the black solid (2) and 0.12 g of dtc_2 were dissolved in 20 mL of DMF, and the solution was stirred at 40 °C for 30 min. A change of the color from black to orange was noted. After the addition of NaI (1 g in 70 mL of MeOH) an orange solid precipitated. Recrystallization from $\text{CH}_2\text{Cl}_2/\text{EtOH}$ gave 0.24 g of $[\text{Mo}_3\text{S}_7(\text{tpy})_2(\text{dtc})]\text{I}$. UV/vis: No maximum above 260 nm. Anal. Calc for $\text{C}_{15}\text{H}_{18}\text{N}_3\text{Mo}_3\text{S}_{13}\text{I}$: C, 17.88; H, 1.80; N, 4.17; Mo, 28.56; I, 12.59. Found: C, 17.98; H, 2.02; N, 4.20; Mo, 28.51; I, 12.33.

Preparation of $(\text{PPh}_4)_2[\text{Mo}_3\text{S}_7(\text{cat})_3]$. $(\text{PPh}_4)_2[\text{Mo}_3\text{S}_7\text{Br}_6]$ (0.5 g) was dissolved in 30 mL of CH_3CN (70 °C). H_2cat (110 mg) and NEt_3 (200 mg in 20 mL of CH_3CN) were then added. The dark reddish brown solution was evaporated to dryness and the residue dissolved in a mixture of DMF (5 mL) and MeOH (10 mL). The solution was heated to 60 °C, and water was added until initial precipitation. After cooling of the mixture to room temperature, the suspension was filtered and the brown solid was washed with MeOH/ H_2O and Et_2O . Yield: 340 mg (75%). Vis (CH_3CN): $\lambda_{\text{max}} = 424 \text{ nm}$, $\epsilon = 1.5 \times 10^4$. Anal. Calc for $\text{C}_{66}\text{H}_{52}\text{Mo}_3\text{O}_6\text{P}_2\text{S}_7$: C, 52.33; H, 3.43; Mo, 19.00. Found: C, 51.76; H, 3.40; Mo, 18.86.

Preparation of $[\text{Mo}_3\text{S}_7(\text{oxq})_3]\text{Br}$. $(\text{NEt}_4)_2[\text{Mo}_3\text{S}_7\text{Br}_6]$ (0.75 g) was dissolved in 80 mL of CH_3CN (70 °C), and Hoxq (1.52 g) was then added. NEt_3 (0.9 g in 15 mL of CH_3CN) was added slowly, and the now red solution was refluxed for 1 h. On cooling of the solution to room temperature, a red solid precipitated. Recrystallization from DMF/ Et_2O gave 550 mg (70%) of the complex. Vis: $\lambda_{\text{max}} = 427 \text{ nm}$, $\epsilon = 1.2 \times 10^4$. Anal. Calc for $\text{C}_{27}\text{H}_{18}\text{N}_3\text{O}_3\text{S}_7\text{Mo}_3\text{Br}$: C, 31.65; H, 1.77; N, 4.10; Mo, 28.09. Found: C, 30.56; H, 1.91; N, 4.23; Mo, 27.85.

X-ray Diffraction Studies of $[\text{Mo}_3\text{S}_7(\text{dtc})_3]\text{I}$. The crystallographic data and measuring parameters of the two modifications, characterized by X-ray analysis, are summarized in Table I. For both crystals, no decay was observed during data collection. The final atomic positional parameters are presented in Table II. Some additional information about the structure solution is given in the following two paragraphs.

Table I. Crystallographic Data for $\text{Mo}_3\text{S}(\text{S}_2)_3(\text{dtc})_3\text{I}$

	modification 1	modification 2
chem formula	$\text{C}_{15}\text{H}_{30}\text{I}\text{Mo}_3\text{N}_3\text{S}_{13}$	
fw	1083.98	
cryst size, mm	$0.07 \times 0.1 \times 0.1$	$0.65 \times 0.27 \times 0.75$
space group	<i>Aba2</i> (No. 41)	<i>Iba2</i> (No. 45)
a, Å	24.92 (2)	17.761 (3)
b, Å	17.93 (1)	24.281 (4)
c, Å	16.56 (1)	16.74 (1)
α , deg	90.0	90.0
β , deg	90.0	90.0
γ , deg	90.0	90.0
V , Å ³	7397 (12)	7220 (7)
Z	8	8
T, °C	22	22
data collec instrument	Picker/Stoe	Enraf Nonius CAD-4
$\lambda(\text{Mo K}\alpha)$, Å		0.710 73
ρ_{calc} , g cm ⁻³	1.95	1.994
μ , cm ⁻¹	25.3	25.88
orientation reflns:	24; $16 \leq 2\theta \leq 24$	25; $21.6 \leq 2\theta \leq 25.4$
no.; range, deg		
$R(F_o)^a$	0.063	0.047
$R_w(F_o)^b$	0.090	0.065

$$^a R = \sum ||F_o| - |F_c|| / \sum |F_o|. \quad ^b R_w = [\sum w(|F_o| - |F_c|)^2 / \sum w|F_o|^2]^{1/2}; w = 1/\sigma^2(|F_o|).$$

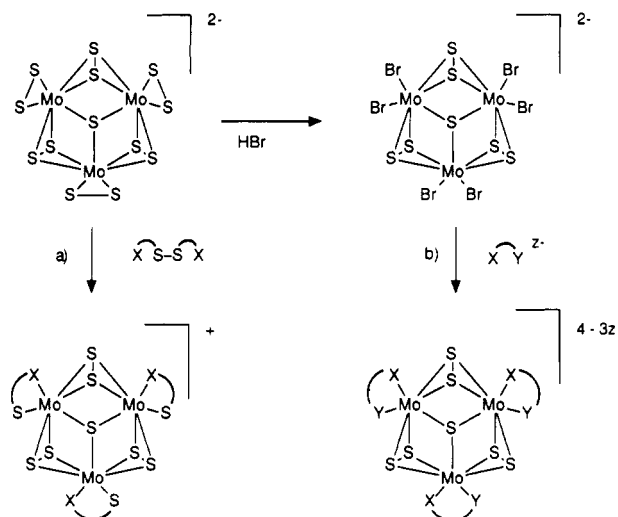
Modification 1. Possible space groups indicated by preliminary precession photographs were *Aba2* and *Cmca*. The noncentrosymmetric one, *Aba2*, was favored because of the typical triangular shape of the crystals and was confirmed by structure analysis. The heavy atoms could be found by interpretation of the Patterson map. The program systems SHELXTL¹³ and XTAL¹⁴ were used for the calculations. The heavy atoms including sulfur could be easily refined in the anisotropic mode. The organic ligands, particularly the ethyl groups, were not quite uniquely localizable. This can be seen in connection with weak satellite reflections near the systematic extinct reciprocal lattice points hkl with $k + l$ odd, corresponding to an incommensurate modulation of the structure. The satellites were observed in precession photographs of large crystals but could hardly be observed with the small crystal used for the intensity measurements. Since the modulated structure was only of marginal interest for the present investigation, the satellite reflections were not further studied. The ethyl carbon atoms could be refined isotropically, but the resulting coordinates give only a rough estimate of the positions and the observed deviations of some distances and angles at carbon and nitrogen atoms from the expected values are not significant. The isotropic temperature factors of dtc should rather be interpreted in terms of the modulation amplitude rather than as thermal motion.

Modification 2 was found to crystallize in the space group *Iba2*. A numerical absorption correction, based on nine indexed crystal faces, was applied with SHELX76;¹⁵ minimum and maximum transmission factors were 0.2397 and 0.5143. The structure was solved with the Patterson interpretation routine of SHELXS86¹⁶ in combination with difference Fourier calculations of SHELX76. After calculation of the H atom positions with SHELX76, the final refinement was carried out with the MOLEN program system.¹⁷ The four carbon atoms and the nitrogen atom of ligand 1 were refined with isotropic displacement parameters. The large values for these atoms and some unusual bond distances and angles again indicate a positional disorder, as already seen for the ligands of modification 1.

Results and Discussion

Preparation Procedures. The synthetic pathways are summarized in Figure 1. Two different methods were used to obtain $\text{Mo}_3\text{S}(\text{S}_2)_3$ complexes:

- (13) Sheldrick, G. M. SHELXTL-Plus 88. Structure Determination Software Programs. Nicolet Inst. Corp., Madison, WI, 1988.
- (14) Hall, S. R.; Stewart, J. M. XTAL 2.6, User's Manual. University of W. Australia and University of Maryland, 1989.
- (15) Sheldrick, G. M. SHELX76. Program for Crystal Structure Determination. University of Cambridge, Cambridge, U.K., 1976.
- (16) Sheldrick, G. M. SHELXS86, Crystal Structure Solution. In *Crystallographic Computing*; Sheldrick, G. M., Krüger, C., Goddard, R., Eds.; Oxford University Press: Oxford, England, 1985; pp 175-189.
- (17) MolEN, An Interactive Structure Solution Procedure. Enraf-Nonius, Delft, The Netherlands, 1990.



In method a the terminal S_2 ligands in $[Mo_3S_7]^{2-}$ were oxidized with activated organic disulfides as 2,2'-dithiodipyridine (tpy_2) and tetraethylthiuram disulfide (dte_2). However, no reaction was observed when disulfides with lower oxidizing power were used, as for example cystine. The monocationic complexes as formed in solution could easily be isolated as the solid iodides by the addition of an excess of NaI to the product solution.

In method b the six bromine atoms in $[Mo_3S_7(S_2)_3Br_6]^{2-}$ were easily substituted by bidentate ligands. Some of the ligands were used in their protonated form. In this case, an excess of ligand and base (triethylamine) must be used to obtain satisfactory yields. The anionic cat complex was isolated as the PPh_4 salt, while the monocationic dtc and oxq complexes were precipitated as the corresponding bromides. The addition of an excess of NaI allowed also the isolation of the iodides. The two $[Mo_3S_7(S_2)_3(dtc)_3]^+$ compounds, obtained as iodides according to method a and as a bromide and iodide according to method b, proved to be identical according to their FAB-MS, 1H NMR, and ^{13}C NMR spectra and X-ray analysis.

Physical Properties and Spectroscopic Characterization. The Mo_3S_7 complexes were obtained as microcrystalline, diamagnetic solids, stable in air and insoluble in water. $[Mo_3S_7(oxq)_3]Br$, $[Mo_3S_7(dtc)_3]Br$, $[Mo_3S_7(dtc)_3]I$, $[Mo_3S_7(tpy)_2(dtc)]I$, and $[Mo_3S_7(tpy)_3]I$ are soluble in $CHCl_3$ and CH_2Cl_2 ; $(PPh_4)_2[Mo_3S_7(cat)_3]$ is soluble in MeOH or DMF. DMSO is an especially good solvent for all obtained compounds. However, in the 1H NMR spectra of the oxq and the cat complexes, measured in DMSO- d_6 , the signals of the free ligands ($\leq 10\%$) could be detected, indicating a partial decomposition of the complex in solution.

All the new compounds are of an intense red, yellow, or brown color. UV/vis spectra of triangular Mo_3 clusters have been discussed and correlated with MO calculations in literature.¹⁸ Müller et al. analyzed the vis spectrum of $[Mo_3S_7(S_2)_6]^{2-}$. The maximum at 558 nm and the shoulder at 540 nm have been assigned to a LMCT transition (465 nm, $\epsilon = 3600$) and a transition within the Mo_3S_7 core (540 nm, $\epsilon = 1100$), respectively. If we consider that the free ligands, used in our investigation, do not absorb in the range 400–700 nm, the observed maxima for the oxq (424 nm) and cat complexes (432 nm) are in agreement with the interpretation as a LMCT similar to the one in $[Mo_3S_7(S_2)_6]^{2-}$ (Figure 2). However, no significant absorbance has been observed above 450 nm for the dtc and tpy complexes. This result disagrees with a general existence of intense transitions for triangular Mo_3 cores in the range 450–700 nm. As already reported previously, the complexes with mercaptosuccinic acid and 2-mercaptobenzoic acid showed no maximum above 350 nm

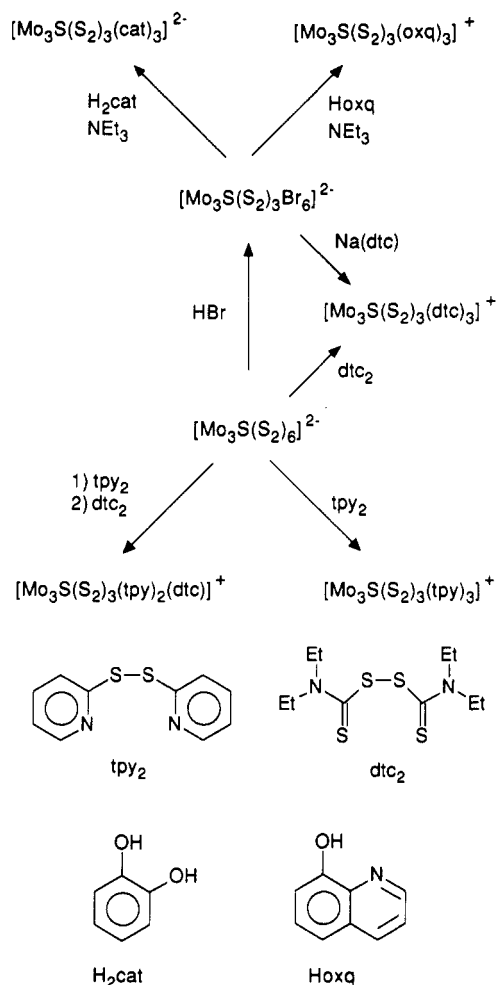


Figure 1. Scheme of synthetic pathways.

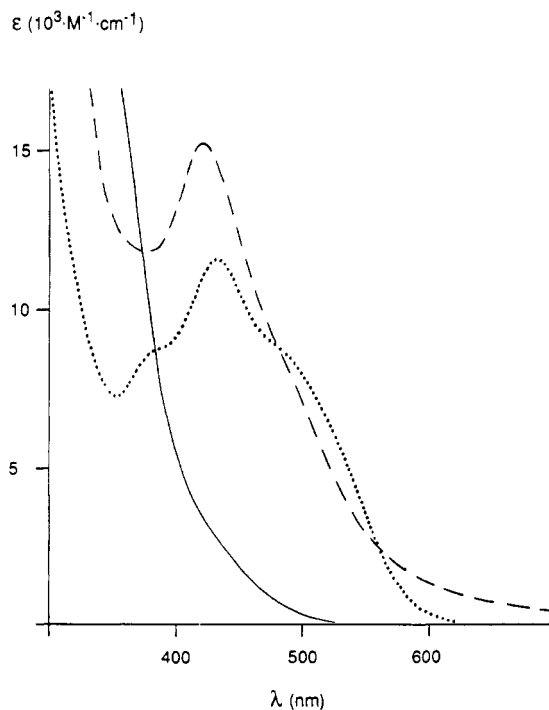


Figure 2. Vis spectra of $(PPh_4)_2[Mo_3S_7(cat)_3]$ (dashed line), $[Mo_3S_7(oxq)_3]Br$ (dotted line), and $[Mo_3S_7(dtc)_3]I$ (solid line).

either.⁹

1H NMR and ^{13}C NMR spectra may be of interest to investigate ligand dissociation or ligand exchange. The coordination of the ligands causes characteristic shifts of the observed signals.

- (18) Müller, A.; Jostes, R.; Jaegermann, W.; Bhattacharyya, R. G. *Inorg. Chim. Acta* **1980**, *41*, 259.
 (19) Fedin, V. P.; Kolesov, B. A.; Mironov, Y. V.; Fedorov, V. Y. *Polyhedron* **1989**, *8*, 2419.

Table II. Atomic Coordinates and Isotropic or Equivalent Isotropic Temperature Factors with Estimated Standard Deviations in Parenthesis for Non-Hydrogen Atoms of $[\text{Mo}_3\text{S}_7(\text{dtc})_3]\text{I}$

atom	modification 1				modification 2			
	x	y	z	$U_{\text{eq}}/U_{\text{iso}}, \text{\AA}^2$	x	y	z	$U_{\text{eq}}/U_{\text{iso}}, \text{\AA}^2$
I	0.3696 (1)	0.2604 (1)	0.0000 (0)	0.043 (1)	0.26360 (4)	0.36948 (3)	0.000	0.0527 (1)
Mo(1)	0.2951 (1)	0.1876 (1)	0.2437 (2)	0.030 (1)	0.16088 (4)	0.30692 (4)	-0.23400 (6)	0.0441 (3)
Mo(2)	0.2984 (1)	0.3390 (1)	0.2429 (2)	0.029 (1)	0.31132 (4)	0.29307 (3)	-0.24547 (6)	0.0369 (1)
Mo(3)	0.2177 (1)	0.2659 (1)	0.1639 (2)	0.031 (1)	0.22731 (5)	0.21966 (3)	-0.16176 (6)	0.0386 (1)
S(1)	0.2832 (3)	0.1130 (4)	0.3674 (5)	0.044 (3)	0.0730 (2)	0.3032 (2)	-0.3489 (3)	0.091 (1)
S(2)	0.3538 (3)	0.0737 (4)	0.2365 (6)	0.044 (3)	0.0622 (2)	0.3793 (2)	-0.2199 (3)	0.084 (1)
S(3)	0.2895 (4)	0.4154 (4)	0.3665 (6)	0.049 (3)	0.3802 (2)	0.2766 (1)	-0.3717 (2)	0.0557 (8)
S(4)	0.3603 (3)	0.4497 (4)	0.2373 (6)	0.049 (3)	0.4323 (1)	0.3452 (1)	-0.2434 (2)	0.0475 (6)
S(5)	0.1218 (3)	0.2697 (6)	0.2003 (6)	0.050 (3)	0.2060 (2)	0.1222 (1)	-0.1970 (2)	0.0584 (8)
S(6)	0.1616 (3)	0.2674 (5)	0.0381 (5)	0.042 (2)	0.2298 (2)	0.1611 (1)	-0.0369 (2)	0.0529 (8)
S(7)	0.3631 (3)	0.2620 (5)	0.3193 (5)	0.041 (2)	0.2428 (2)	0.3673 (1)	-0.3154 (2)	0.0521 (6)
S(8)	0.2169 (3)	0.1273 (4)	0.1794 (5)	0.042 (3)	0.0892 (2)	0.2343 (1)	-0.1639 (2)	0.0574 (8)
S(9)	0.2223 (3)	0.4045 (5)	0.1756 (6)	0.047 (3)	0.3644 (2)	0.2082 (1)	-0.1854 (2)	0.0523 (6)
S(10)	0.3703 (3)	0.2604 (4)	0.1968 (5)	0.034 (2)	0.2523 (1)	0.3743 (1)	-0.1930 (2)	0.0405 (5)
S(11)	0.2735 (3)	0.1718 (4)	0.1027 (6)	0.036 (2)	0.1514 (1)	0.2860 (1)	-0.0924 (2)	0.0441 (6)
S(12)	0.2773 (3)	0.3548 (4)	0.1015 (6)	0.035 (2)	0.3332 (1)	0.2689 (1)	-0.1071 (2)	0.0400 (5)
S(13)	0.2308 (3)	0.2663 (4)	0.3059 (5)	0.036 (2)	0.2201 (2)	0.2334 (1)	-0.3026 (2)	0.0517 (6)
C(11)	0.330 (1)	0.050 (1)	0.335 (2)	0.032 (6)	0.020 (2)	0.380 (1)	-0.303 (3)	0.23 (1)
N(1)	0.347 (1)	-0.010 (2)	0.372 (2)	0.052 (7)	-0.026 (1)	0.3816 (7)	-0.361 (1)	0.132 (6)
C(12)	0.325 (1)	-0.016 (2)	0.456 (2)	0.048 (8)	-0.046 (1)	0.3663 (9)	-0.439 (1)	0.138 (9)
C(13)	0.385 (2)	-0.062 (2)	0.344 (3)	0.07 (1)	-0.068 (2)	0.434 (1)	-0.343 (2)	0.20 (1)
C(14)	0.366 (2)	0.024 (3)	0.527 (4)	0.12 (2)	-0.004 (2)	0.395 (1)	-0.496 (2)	0.20 (1)
C(15)	0.442 (2)	-0.058 (3)	0.352 (4)	0.11 (2)	-0.116 (2)	0.434 (1)	-0.285 (2)	0.24 (1)
C(21)	0.335 (2)	0.474 (2)	0.320 (2)	0.057 (9)	0.4489 (6)	0.3221 (4)	-0.3396 (6)	0.047 (3)
N(2)	0.359 (2)	0.533 (2)	0.374 (3)	0.07 (1)	0.5065 (5)	0.3378 (4)	-0.3835 (5)	0.048 (3)
C(22)	0.341 (2)	0.539 (2)	0.465 (3)	0.07 (1)	0.5158 (8)	0.3199 (5)	-0.4636 (7)	0.067 (4)
C(23)	0.408 (3)	0.586 (3)	0.347 (5)	0.14 (2)	0.5645 (7)	0.3732 (6)	-0.3500 (8)	0.067 (4)
C(24)	0.368 (2)	0.497 (2)	0.524 (3)	0.07 (1)	0.497 (1)	0.3604 (6)	-0.5267 (9)	0.084 (4)
C(25)	0.484 (3)	0.564 (4)	0.360 (6)	0.20 (3)	0.548 (1)	0.4318 (6)	-0.356 (1)	0.104 (5)
C(31)	0.107 (1)	0.274 (2)	0.096 (2)	0.039 (7)	0.2123 (6)	0.1052 (4)	-0.0972 (7)	0.048 (3)
N(3)	0.06 (1)	0.281 (2)	0.074 (2)	0.058 (8)	0.2062 (7)	0.0548 (4)	-0.0713 (7)	0.068 (3)
C(32)	0.009 (2)	0.291 (2)	0.131 (3)	0.07 (1)	0.190 (1)	0.0090 (4)	-0.1276 (8)	0.081 (3)
C(33)	0.043 (1)	0.286 (2)	-0.011 (2)	0.053 (9)	0.217 (1)	0.0413 (6)	0.013 (1)	0.113 (6)
C(34)	0.000 (2)	0.369 (2)	0.148 (4)	0.10 (2)	0.108 (1)	-0.0020 (7)	-0.134 (1)	0.101 (5)
C(35)	0.039 (2)	0.215 (3)	-0.036 (4)	0.11 (2)	0.284 (2)	0.029 (1)	0.043 (2)	0.29 (1)

$$^a U_{\text{eq}} = \frac{1}{3} \sum_i \sum_j U_{ij} a_i^* a_j^* a_i a_j$$

Table III. Summarized IR Data for $[\text{Mo}_3\text{S}(\text{S}_2)_3\text{L}_3]$ Complexes Including Selected Characteristic Vibrations (cm^{-1}) of the $\text{Mo}_3\text{S}(\text{S}_2)_3$ Core in Correlation with the Assignments from Refs 8 and 19

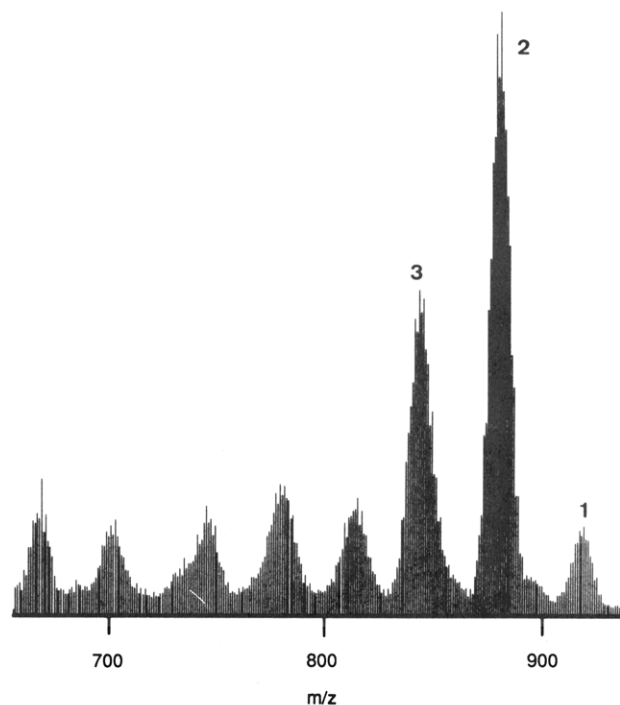
complex	ν_1	ν_2	ν_3	ν_4
$[\text{Mo}_3\text{S}_7(\text{oxq})_3]^+$	569	441	391	270
$[\text{Mo}_3\text{S}_7(\text{dtc})_3]^+$	524	475	373	285
$[\text{Mo}_3\text{S}_7(\text{tpy})_3]^+$	513	465	399	294
$[\text{Mo}_3\text{S}_7(\text{tpy})_2(\text{dtc})]^+$	515	462	400	288
$[\text{Mo}_3\text{S}_7(\text{cat})_3]^{2-}$	529	455	390 (sh)	264
reference	$\nu(\text{S}_{\text{ax}}-\text{S}_{\text{eq}})$	$\nu(\text{Mo}-\mu_3-\text{S})$	$\nu(\text{Mo}-\text{S}_{\text{ax}})$	$\nu(\text{Mo}-\text{S}_{\text{eq}})$
$[\text{Mo}_3\text{S}(\text{S}_2)_6]^{2-}$	546	462	388	271 ^a
$[\text{Mo}_3\text{S}_7\text{Cl}_6]^{2-}$	560/566	461	392	284 ^b

^a Reference 19. ^b Reference 8.

In addition, the coordination of C_{2v} ligands is accompanied by the loss of their symmetry, indicated in the ^{13}C NMR spectrum by the appearance of six peaks for the coordinated cat molecule (161.5, 158.3, 116.5, 113.43, 113.39, 112.1 ppm) and five peaks for the coordinated dtc molecule (202.2, 45.1, 44.7, 12.8, 12.6 ppm). As observed for many dithiocarbamates and indicated by the short C–N bond, rotation around this bond is slow in terms of the NMR time scale, which allows the observation of two distinct diastereotopic ethyl groups.

The IR spectra of the four compounds were dominated by the peaks from the coordinated ligands. The vibrations of the cluster core appeared in the range of 200–600 cm^{-1} and are summarized in Table III. However, the rather low intensities of these bands provided only limited information about composition or structure of the obtained compounds.

FAB mass spectra confirmed the proposed trinuclear structure of these complexes. The observed characteristic isotope multiplets, caused by the polyisotopic nature of Mo and S, allowed an unambiguous assignment of the detected signals. The spectra of the

**Figure 3.** FAB⁺ mass spectrum of $[\text{Mo}_3\text{S}_7(\text{tpy})_2(\text{dtc})]\text{I}$: (1) $[\text{Mo}_3\text{S}_7(\text{tpy})(\text{dtc})_2]^+$; (2) $[\text{Mo}_3\text{S}_7(\text{tpy})_2(\text{dtc})]^+$; (3) $[\text{Mo}_3\text{S}_7(\text{tpy})_3]^+$.

cat, oxq, and dtc complexes have been discussed earlier.¹¹ The FAB⁺ spectrum of the tpy complex is analogous to that of other monocationic complexes with $[\text{Mo}_3\text{S}_x(\text{tpy})_3]^+$ ($7 \geq x \geq 4$) and $[\text{Mo}_3\text{S}_x(\text{tpy})_2]$, ($7 \geq x \geq 5$) as the major fragmentation series

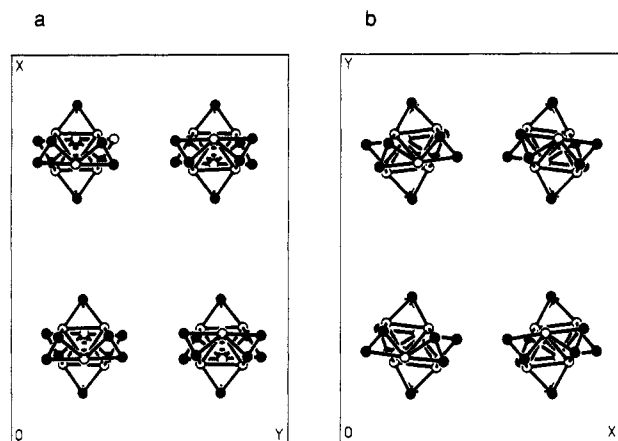


Figure 4. Projection along axis *c* of the unit cells of $[\text{Mo}_3\text{S}_7(\text{dtc})_3]\text{I}$: (a) modification 1; (b) modification 2. Only the $\text{Mo}_3\text{S}(\text{S}_2)_3$ cores are shown for clarity. The sulfur atoms are shown as solid circles; Mo atoms are shown as open circles.

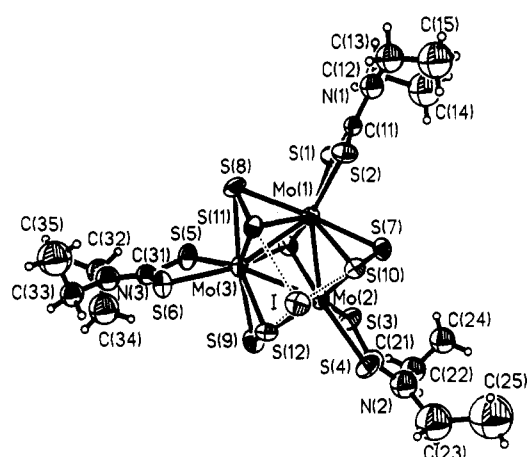


Figure 5. Drawing of $[\text{Mo}_3\text{S}_7(\text{dtc})_3]\text{I}$ (modification 1) with numbering scheme and vibrational ellipsoids at the 50% probability level.

whereas in the spectrum of $[\text{Mo}_3\text{S}(\text{S}_2)_3(\text{tpy})_2(\text{dtc})]\text{I}$ the ions $[\text{Mo}_3\text{S}_7(\text{tpy})_3]^+$, $[\text{Mo}_3\text{S}_7(\text{tpy})_2(\text{dtc})]^+$, and $[\text{Mo}_3\text{S}_7(\text{tpy})(\text{dtc})_2]^+$ were detected (Figure 3), indicating reversible ligand-exchange reaction. It should be noted that a corresponding reaction in solution is not to be expected. Actually, no dissociation of dtc has been observed in solution at room temperature. In the ^1H and ^{13}C NMR spectra of the dtc complex, the free ligand has never been detected.

Structure of $[\text{Mo}_3\text{S}(\text{S}_2)_3(\text{dtc})_3]\text{I}$. Two different types of crystals were obtained either by crystallization from CH_2Cl_2 /hexane (modification 1) or DMF/ether (modification 2). Modification 1 crystallized in a base-centered lattice (space group *Aba2*) whereas modification 2 crystallized in a body-centered lattice (space group *Iba2*). The molecules of both modifications were almost identical. Also the packing of the molecules was similar for both modifications. A projection of the unit cells of the two modifications is presented in Figure 4. If the cell is viewed along axis *c*, four molecules are located in the corners of a rectangle. Another set of four molecules lies approximately below the corners of this rectangle. However, in modification 2 (Figure 4b), the molecules are slightly twisted against each other. This twisting allowed a somewhat more dense packing as seen by a smaller value for the unit cell volume and a higher value for the density respectively. A drawing of the molecule with the numbering scheme is given in Figure 5. The three Mo atoms form an approximately equilateral triangle with average Mo–Mo distances of 2.73 Å (modification 1) or 2.71 Å (modification 2), respectively, and are capped by the single μ_3 -S atom. Each Mo atom is coordinated to one dtc ligand, forming a four-membered ring, which is oriented approximately perpendicular to the triangle of the three Mo atoms. A summary of selected bond lengths and angles is given in Tables

Table IV. Summarized Bond Lengths (Å) of the Mo_3S_{13} Entities in the Two Modifications of $[\text{Mo}_3\text{S}_7(\text{dtc})_3]\text{I}$ with Estimated Standard Deviations in Parentheses

bond	modification 1		modification 2	
	av value	range	av value	range
Mo–Mo	2.726	2.716 (4)–2.733 (5)	2.708	2.700 (1)–2.714 (1)
Mo– μ_3 -S	2.372	2.370 (8)–2.375 (9)	2.376	2.368 (3)–2.385 (3)
Mo–S _{eq}	2.487	2.470 (9)–2.499 (8)	2.476	2.469 (3)–2.482 (3)
Mo–S _{ax}	2.411	2.403 (8)–2.42 (1)	2.411	2.400 (3)–2.430 (3)
Mo–S _{cis}	2.468	2.465 (9)–2.47 (1)	2.474	2.468 (3)–2.478 (3)
Mo–S _{trans}	2.513	2.507 (8)–2.515 (8)	2.505	2.494 (3)–2.528 (3)
S _{eq} –S _{ax}	2.050	2.04 (1)–2.06 (1)	2.056	2.048 (4)–2.063 (5)

Table V. Summarized Bond Angles (deg) of the Mo_3S_{13} Entities in the Two Modifications of $[\text{Mo}_3\text{S}_7(\text{dtc})_3]\text{I}$ with Estimated Standard Deviations in Parentheses

angle	modification 1		modification 2	
	av value	range	av value	range
Mo–Mo–Mo	60.0	59.7 (1)–60.3 (1)	60.00	59.70 (3)–60.23 (3)
S _{ax} –Mo–S _{ax}	85.7	85.6 (3)–85.9 (3)	85.3	84.9 (1)–85.5 (1)
S _{ax} –Mo–S _{cis}	133.2	131.0 (3)–135.8 (3)	133.1	131.4 (1)–134.9 (1)
S _{ax} –Mo–S _{eq}	49.4	49.0 (3)–49.8 (3)	49.7	49.4 (1)–50.1 (1)
S _{ax} –Mo–S _{trans}	134.8	134.5 (3)–135.3 (3)	134.7	134.3 (1)–135.2 (1)
S _{cis} –Mo–S _{trans}	89.2	88.5 (3)–90.2 (3)	88.5	87.2 (1)–90.4 (1)
S _{cis} –Mo–S _{eq}	70.1	69.4 (3)–70.6 (3)	70.3	70.0 (2)–70.6 (1)
S _{eq} –Mo–S _{cis}	89.6	86.8 (3)–92.3 (3)	89.5	88.0 (1)–91.4 (1)
S _{eq} –Mo–S _{trans}	170.4	169.4 (3)–171.2 (3)	170.4	169.8 (1)–170.8 (1)
S _{eq} –Mo–S _{eq}	94.4	93.5 (3)–95.3 (3)	94.3	92.7 (1)–96.3 (1)
μ_3 -S–Mo–S _{ax}	109.9	109.7 (3)–110.3 (3)	110.5	110.3 (1)–110.7 (1)
μ_3 -S–Mo–S _{cis}	83.3	82.9 (3)–83.8 (3)	83.5	82.8 (2)–83.9 (1)
μ_3 -S–Mo–S _{eq}	85.2	84.4 (3)–86.0 (3)	85.2	84.9 (1)–85.5 (1)
μ_3 -S–Mo–S _{trans}	153.4	152.3 (3)–154.0 (3)	153.7	152.8 (2)–154.6 (1)
Mo–S _{ax} –Mo	68.8	68.7 (2)–68.9 (3)	68.3	68.25 (8)–68.38 (7)
Mo–S _{ax} –S _{eq}	67.2	66.5 (3)–67.5 (3)	66.8	66.3 (1)–67.1 (1)
Mo–S _{eq} –Mo	66.5	66.4 (2)–66.6 (2)	66.3	66.20 (8)–66.36 (8)
Mo–S _{eq} –S _{ax}	63.4	63.0 (3)–63.6 (3)	63.5	63.1 (1)–64.1 (1)
Mo– μ_3 -S–Mo	70.1	69.9 (2)–70.3 (2)	69.5	69.40 (9)–69.56 (9)

IV and V. For the $\text{Mo}_3\text{S}_{13}\text{I}$ part, the deviation from C_{3v} symmetry is only small, which obviously is the relevant symmetry for the entire complex in solution according to the ^{13}C and ^1H NMR spectra. The structure of the cluster core corresponds closely to those found in other $\text{Mo}_3\text{S}(\text{S}_2)_3$ complexes,^{2–5,7} however, special attention should be given to the iodine atom, which forms a tetrahedron together with the axial S atoms of the three disulfido bridges. The average I–S distances of 3.30 Å (modification 1) and 3.25 Å (modification 2) are significantly shorter than the sum of the van der Waals radii (4.0 Å), indicating a weak binding of iodine by the three S atoms. It should be noted that this binding is found in both modifications. Thus, it seems rather unlikely that this particular arrangement is a consequence of the packing in the crystal.

Conclusions

$[\text{Mo}_3\text{S}(\text{S}_2)_6]^{2-}$ is an instructive model for the different reactivity of bridging and terminal disulfido groups. The results of this investigation, together with other observations, clearly demonstrate that the terminal S_2 entities react rather with electrophilic or oxidizing agents,^{8,9} while the bridging S_2 entities are selectively attacked by reducing or nucleophilic agents.^{6,10,20} Fedin et al. found a decrease $\text{Cl}_2 > \text{Br}_2 \gg \text{I}_2$ for the easiness of oxidation.⁸ This trend suggests a direct dependence of the reaction rate on the redox potential of the oxidizing agent. Little systematic data are known on the accurate reduction potentials of organic disulfides. However, the sequence dtc_2 ($E^\circ = -0.06$ V) $>$ tpy_2 $>$ cystine ($E^\circ = -0.34$ V, pH 7) has been established.²¹ Hence,

- (20) Hegetschweiler, K.; Keller, T.; Bäuml, M.; Rihs, G.; Schneider, W. *Inorg. Chem.*, following paper in this issue.
- (21) (a) Akers, H. A.; Vang, M. C.; Updike, T. D. *Can. J. Chem.* **1987**, *65*, 1364 and references therein. (b) Nichols, P. J.; Grant, M. W. *Aust. J. Chem.* **1982**, *35*, 2455. (c) Antelo, J. M.; Arce, F.; Rey, F.; Sastre, M. *Electrochim. Acta* **1985**, *30*, 927. (d) Loach, P. A. In *Handbook of Biochemistry*; Sober, H. A., Ed.; The Chemical Rubber Co.: Cleveland, OH, 1968; p J-27.

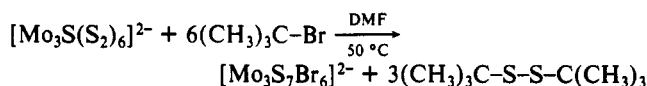
Table VI. Summary of Selected Structural Data (Average Distances in Å) for Symmetrically Coordinated $\text{Mo}_3\text{S}(\text{S}_2)_3\text{X}_6$ Complexes, Where X Represents Either a Monodentate Ligand or a Ligand Atom of a Symmetric Bidentate Ligand and Y Represents the Anion, Coordinated by the Three Axial Sulfur Atoms of the Complex

ligand	Mo-X _{cis}	Mo-X _{trans}	Mo-S _{eq}	Mo-S _{ax}	Mo-μ ₃ -S	Y	S _{ax} -Y	ref
dtc ⁻	2.47	2.51	2.50	2.41	2.37	I ⁻	3.30	a
dtc ⁻	2.47	2.51	2.48	2.41	2.38	I ⁻	3.25	b
(EtO) ₂ PS ₂ ⁻	2.50	2.55	2.48	2.40	2.37	Cl ⁻	2.90	c
Et ₂ PS ₂ ⁻	2.51	2.56	2.49	2.40	2.38	Et ₂ PS ₂ ⁻	3.08	d
S ₂ ²⁻	2.41	2.46	2.49	2.42	2.35			e
Cl ⁻	2.46	2.50	2.48	2.39	2.35	Cl ⁻	2.94	f
Cl ⁻	2.48	2.51	2.50	2.40	2.36			g

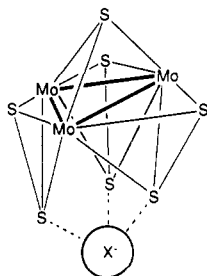
^aThis work, modification 1. ^bThis work, modification 2. ^cReference 5. ^dReference 4. ^eReference 3. ^fReference 7. ^gReference 2.

the observed reactivity $\text{dtc}_2 > \text{tpy}_2 \gg \text{cystine}$ for the oxidation with organic disulfides indicates again the influence of the redox potential on the reaction rate. On the other hand, it is noteworthy that the disulfides are much weaker oxidizing agents than the halogens used by Fedin. Thus, it is obvious that the rate of oxidation cannot be explained simply in terms of the redox potential only.

Seemingly, the reaction of $[\text{Mo}_3\text{S}(\text{S}_2)_6]^{2-}$ with HBr must be rather considered as the attack of the electrophile H^+ than as the simple substitution of the coordinated S_2^{2-} by Br^- . In agreement with this postulate, we found that $[\text{Mo}_3\text{S}(\text{S}_2)_3\text{Br}_6]^{2-}$ is easily obtained by the reaction of $[\text{Mo}_3\text{S}(\text{S}_2)_6]^{2-}$ with alkyl bromides according to the equation



Considering the degradation of the bridging disulfido groups by nucleophilic agents, the binding of iodine to the three axial sulfur atoms in the dtc complex is particularly interesting. A similar interaction has been described for Cl^- in $[\text{Mo}_3\text{S}(\text{S}_2)_3((\text{EtO})_2\text{PS}_2)_3]\text{Cl}$,⁵ $[\text{Mo}_3\text{S}(\text{S}_2)_3\text{Et}_2\text{PS}_2]\text{Cl}$,²² and $(\text{NEt}_4)_3[\text{Mo}_3\text{S}(\text{S}_2)_3\text{Cl}_6]\text{Cl}$.⁷



In $\text{M}_2[\text{Mo}_3\text{S}_7(\text{Hmsa})_3][\text{Mo}_3\text{S}_7(\text{Hmsa})_2\text{msa}]\text{Br}\cdot 6\text{H}_2\text{O}$,²³ Br^- is coordinated by the six sulfur atoms of two $\text{Mo}_3\text{S}(\text{S}_2)_3$ entities,⁹ and in $[\text{Mo}_3\text{S}(\text{S}_2)_3(\text{Et}_2\text{PS}_2)_3](\text{Et}_2\text{PS}_2)$, a short distance between the axial sulfur atoms of the complex and the sulfur atom of the ionic Et_2PS_2^- entity has been reported (Table VI).⁴ Hence, it seems reasonable to assume that the three axial sulfur atoms of the $[\text{Mo}_3\text{S}(\text{S}_2)_3]$ core acted as an anionic binding site. It is tempting to regard this anion binding as a first step of the nucleophilic attack on the bridging disulfido groups. However, this hypothesis is not quite in agreement with the results of Fedin et al., who postulated that the equatorial sulfur atoms are eliminated predominantly.⁸

Nothing is known so far about the stability of such anion- $[\text{Mo}_3\text{S}(\text{S}_2)_3]$ interactions. It should be noted that in the FAB mass spectrum of the dtc complex only the dissociated species

$[\text{Mo}_3\text{S}_x(\text{dtc})_3]^+$ with $7 \geq x \geq 4$ and $[\text{Mo}_3\text{S}_x(\text{dtc})_2]^+$ with $7 \geq x \geq 5$ have been detected. However, in the spectrum of the oxq complex, an ion assignable to $[\text{Mo}_3\text{S}_7(\text{oxq})_3\text{Br}]^+$ has been found.¹¹ The strength of this anion binding in solution can be elucidated by cryoscopic, ebullioscopic, or conductivity measurements. A subsequent investigation including a variety of anions and $\text{Mo}_3\text{S}(\text{S}_2)_3$ complexes is in progress and will be published elsewhere.

Finally, we focus attention on the binding of the ligands to the cluster core. In both modifications, the distance of the Mo-S bond located trans to the μ_3 -S atom is significantly longer than the bond length to the corresponding atom in the cis position. On the other hand, the Mo- μ_3 -S distance is the shortest of all the Mo-S bond lengths found in the complex. A review of X-ray structures reported in the literature confirmed this result as a general property of the $\text{Mo}_3\text{S}(\text{S}_2)_3$ core (Table VI). Also, the asymmetric binding of the μ_2 -disulfido bridges with a significantly shorter bond length for Mo-S_{ax} compared to Mo-S_{eq} has been generally reported for the Mo_3S_7 core.

The different signals for the free and the coordinated ligand molecules in the NMR spectrum allowed a quantitative determination of the amount of ligand dissociation. According to these results, cat and oxq seemed to be much more labile than dtc. It has been reported elsewhere that no exchange of the coordinated ligand with the counterion X has been observed for $[\text{Mo}_3\text{S}(\text{S}_2)_3(\text{Et}_2\text{PS}_2)_3]\text{X}$, X = dtc, Me_2PS_2 , and Ph_2PS_2 .²⁴ Therefore, there is evidence that in solution chemistry Mo-S bonds are generally more inert compared to Mo-O or Mo-N bonds as present in the oxq or cat complex.

Acknowledgment. A detailed analysis of the electron density distribution of the methyl groups supporting the model of a modulated superstructure of modification 1 was worked out by students of a practical course in crystal structure analysis at the ETH, Zürich, Switzerland. This valuable help of A. Currao, M. Hunziker, Th. Müller, M. Pirotta, and S. Seefeld is gratefully acknowledged. We thank Ruth Blumer and Urs Bucher for the measurement of the NMR spectra and the Swiss National Science Foundation for financial support.

Registry No. $(\text{NH}_4)_2[\text{Mo}_3\text{S}(\text{S}_2)_6]$, 67031-31-6; $(\text{PPh}_4)_2[\text{Mo}_3\text{S}_7\text{Br}_6]$, 127205-35-0; $(\text{NEt}_4)_2[\text{Mo}_3\text{S}_7\text{Br}_6]$, 127294-35-3; $[\text{Mo}_3\text{S}_7(\text{dtc})_3]\text{I}$, 132374-54-0; $[\text{Mo}_3\text{S}_7(\text{dtc})_3]\text{Br}$, 136523-50-7; $[\text{Mo}_3\text{S}_7(\text{tpy})_3]\text{I}$, 136523-51-8; $[\text{Mo}_3\text{S}_7(\text{tpy})_2(\text{dtc})]\text{I}$, 136523-52-9; $(\text{PPh}_4)_2[\text{Mo}_3\text{S}_7(\text{cat})_3]$, 132374-53-9; $[\text{Mo}_3\text{S}_7(\text{oxq})_3]\text{Br}$, 132374-51-7; Mo, 7439-98-7.

Supplementary Material Available: Tables SI-SV, listing crystallographic data, anisotropic displacement parameters, positional parameters of hydrogen atoms, and bond distances and angles, and Figures S1-S3, showing two stereoviews of the unit cell for modification 1 and modification 2 and the FAB⁺ mass spectrum of $[\text{Mo}_3\text{S}_7(\text{tpy})_3]\text{I}$ (16 pages); two tables of calculated and observed structure factors for modification 1 and modification 2 (57 pages). Ordering information is given on any current masthead page.

(22) Mootz, D.; Wiskemann, R.; Wunderlich, H. To be published.

(23) M = $[\text{C}_{18}\text{H}_{30}\text{N}_3]^{3+}$; H₃msa = 2-mercaptosuccinic acid.

(24) Keck, H.; Kuchen, W.; Mathow, J. Z. *Anorg. Allg. Chem.* **1986**, 537, 123.